MINERAL COMPOSITION OF ARARIPE BLACK SHALE BY X-RAY MICROCT

Endyara de Morais Cabral [1]; Isis da Silva Rodrigues[1]; Leyllanne Renalle Batista de Almeida[1]; José Agnelo Soares[1]
Universidade Federal de Campina Grande

Abstract

The Araripe Basin is the largest basin in the interior of the Northeast Brazil, located in the border region of the states of Ceará, Pernambuco and Piauí, and has a huge influence on the climate and in the local economy. Well known for its paleontological occurrences, this basin has also become the target of research aimed at knowing the potential of its rocks as generators or as reservoirs of hydrocarbons. For the accomplishment of this paper 4 samples of black shales extracted from "gypsum" mines, in Ipubi member of the Santana Formation, were used in order to characterize their petrophysical properties, which are still little known. These properties are determined for subsamples through the analysis of x-ray microCT images, and include mineral and organic composition and apparent and actual grain density. In general, the analysis indicated a high content of organic matter, evidencing the hydrocarbon potential of these shales. Thus, computational petrophysics is shown as an important characterization tool for the study of these black shales.

Introduction

The Araripe Basin is located in the region around Ceará, Pernambuco and Piauí states, in the interior of Northeast Brazil. It is the largest basin of the interior of the region covering the plateau of Araripe and the Cariri valley, in approximately 9,000 km². Recognized for the paleontological importance, due to the spectacular occurrences of well-preserved fossils, this basin has also become the target of research aimed at knowing the potential of its rocks as oil generators or as reservoirs of hydrocarbons (Chagas, 2006).

Over time, and throughout the world, oil reservoirs have been increasingly exploited, which are commonly associated with sandstone or carbonate rocks and are called conventional reservoirs. However, given the current high energy demand and the importance of oil production in this context, another type of reservoir has shown an increasing influence in the production scenario, mainly in the United States of America: non-conventional reservoirs.

In the conventional petroleum system, the maturation of the kerogen inside the source rocks gives origin to the hydrocarbons. Then, migration of these hydrocarbons occurs to the interior of a reservoir rock, where they are stored. This accumulation of hydrocarbons occurs thanks to the presence of rocks with sealant characteristics above the reservoir rock and the existence of traps. The same does not happen in an unconventional system, where the source rock is also the reservoir rock of hydrocarbons. Among the unconventional reservoirs, shales are the most commonly encountered type, and due to the low values of porosity and permeability associated, they do not naturally produce at economic rates (Ribeiro, 2015).

A previous study by Batista & Soares (2016) analyzed 21 samples of bituminous shales from the Araripe Basin extracted from outcrops in gypsum and limestone mines on the Ipubi member of the Santana Formation, in the Araripe Basin. These samples were naturally saturated with oil and were subjected to conventional petrophysical tests, in order to determine, among other properties, the grain density. A better knowledge of the mineralogical composition for some samples, which presented a distinct behavior with regard to the densities, was needed. Then, four samples were selected, which were subjected to x-ray microtomography characterization methods for comparison with the results of conventional tests.

The aim of this paper is to investigate the petrophysical properties of these black shale samples in order to evaluate their potential as a source rock and also as an unconventional hydrocarbon reservoir by determining their mineral and organic composition and some of their properties obtained by microtomographic image analysis. In addition, a comparison is made with the conventional petrophysical characterization performed by Batista & Soares (2016).

Method

For the accomplishment of this study, the software Avizo Fire version 8.1 was used for the visualization and exploration of four microCT subsample images with the purpose of obtaining the necessary information.

In order to calculate the grain density of each sub-sample, it was necessary to know the mineral and organic composition and the volumetric fractions related to each material phase present. Therefore, the set of microCT images was initially loaded and to this file was added the Ortho Slice tool, which allows for slices visualization in the software. Subsequently, a subvolume was extracted from the image with the use of the Extract Subvolume tool, with the purpose of delimiting an area of the subsample to be studied, avoiding the edge effect and making the computational processing easier, as shown in Figure (1).

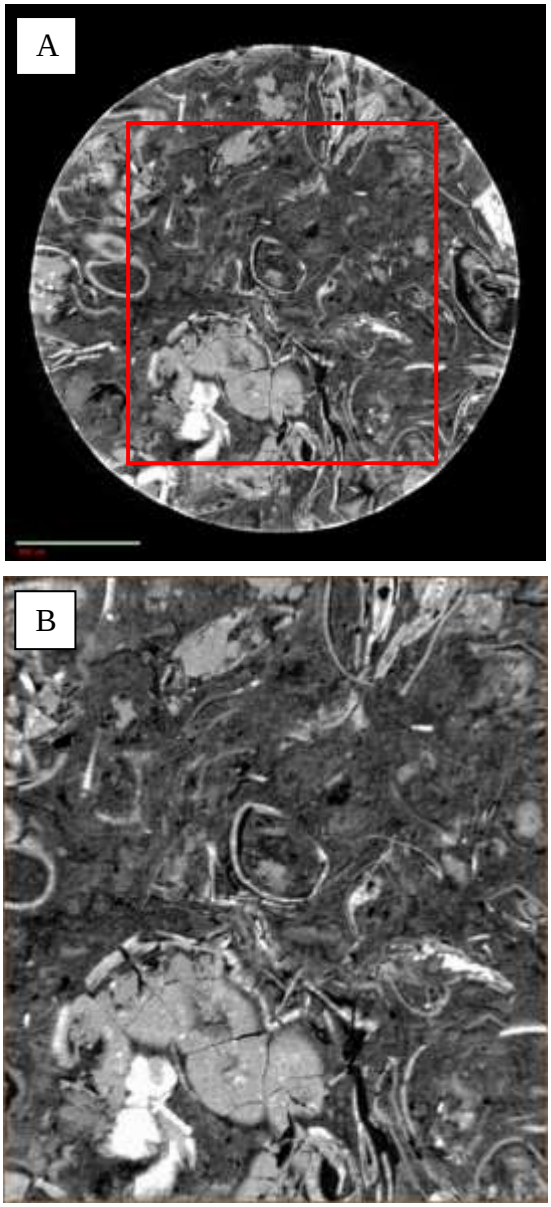

Figure 1: (A) MicroCT image of sample AS_2 visualized with the Ortho Slice tool. (B) Image of subvolume extracted using the tool Extract Subvolume.

Then the image was segmented using the Multi-Thresholding tool, which allowed the determination of a gray tone threshold that separates the components of the mineral matrix, organic matter and pores, based on the different shades of gray in the images. For the visualization and verification of the separated phases, in different colors, the Ortho Slice tool was used again. Figure (2) exemplifies the visualization of the separate phases of sub-sample SA_2.

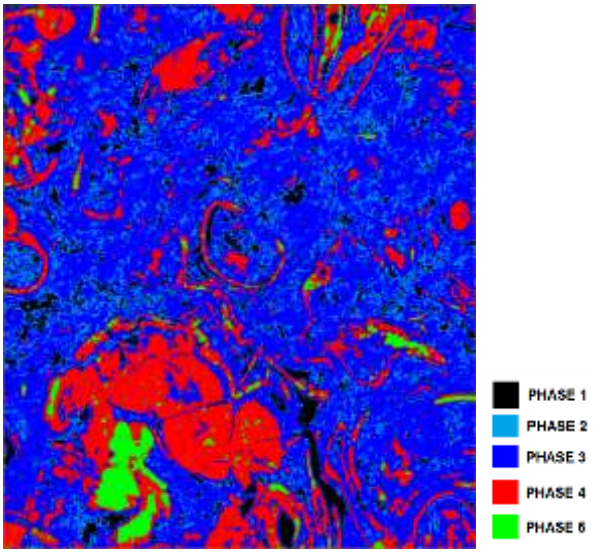

Figure 2: The 5 phases separated by the Multi-Thresholding tool.

After the separation of the gray tones belonging to the different phases in the microtomography images of the subsamples, the present phases are identified, considering the typical composition of the bituminous shale, the shape of the phases, the types of occurrences of the possible minerals, their densities and the associations between them.

This step starts with determining the representative gray tone for the elements in each subsample. A histogram with the frequencies of all shades of gray is generated by the Material Statistics tool, which allows an analysis of the gray tone that best represents each of the previously separated phases.

Regarding mineral composition, at least 3 elements need to be recognized in microtomographic images: pore and 2 mineral components. Thus, the representative gray shades of these 3 elements were used, whose densities are previously known. From these three determined points, the function of nonlinear regression adjustment was obtained that corresponds to the relation between the densities and gray tones predominant in the identified phases (Porto, 2015).

For the phases of unknown composition, the estimated gray tone was applied to the function described by the known phases, allowing the determination of the densities.

Figure (3) exemplifies a density versus representative gray tone graph, where the points relating to the known elements were plotted for the construction of the nonlinear function, making it possible to identify the density of unknown (estimated) phases.

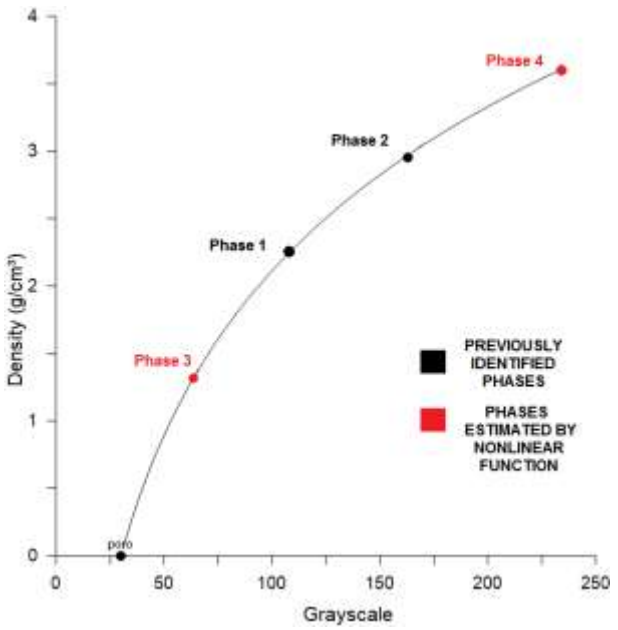

Figure 3: Example of graph for the identification of unknown phases.

To quantify the pixels related to each phase, the Material Statistics tool is used again. In addition to the previously mentioned utility, this function allows to know the count of pixels existing in each of subsample phases.

This step is necessary for the quantification of the elements (identified and estimated) volumetric fractions, since a pixel corresponds to a unit area of a given material in the subsample. This implies that the pixels total count in each phase is proportional to its volume within the analyzed sample. The volumetric fraction of a given phase can be determined as the ratio between the number of pixels of that phase and the subsample total number of pixels.

The volumetric fractions and densities of the phases, allowed the calculation of the grain densities for the four subsamples from Equations (1) and (2), which consider the presence of four solid phases. Phase 1 (pores), because of its negligible density, is not considered in these equations.

$$\rho_{GA} = (Fv_2\rho_2) + (Fv_3\rho_3) + (Fv_4\rho_4) + (Fv_5\rho_5) \quad (1)$$

$$\rho_{GR} = (Fv_3'\rho_3) + (Fv_4'\rho_4) + (Fv_5'\rho_5) \quad (2)$$

where ρ_{GA} is the apparent grain density and ρ_{GR} is the actual grain density, the terms ρ_2, ρ_3, ρ_4 and ρ_5 are the densities of each solid phase. The terms Fv_2, Fv_3, Fv_4 e Fv_5 are the volumetric fractions of the non-porous phases. For equation (2) the volumetric fractions of the mineral phases are recalculated excluding the relative contribution to the organic matter (phase 2), in such a way that the volumetric fractions of each mineral phase become higher than the mineral phases used in Eq. (1), resulting in higher values for the actual grain density.

Results

Graphs of density versus gray tone representative of the phases, with the function of non-linear adjustment were generated (Figure 4), and the coefficient of determination (R^2) in each of the models generated for the 4 subsamples are shown in Table (1).

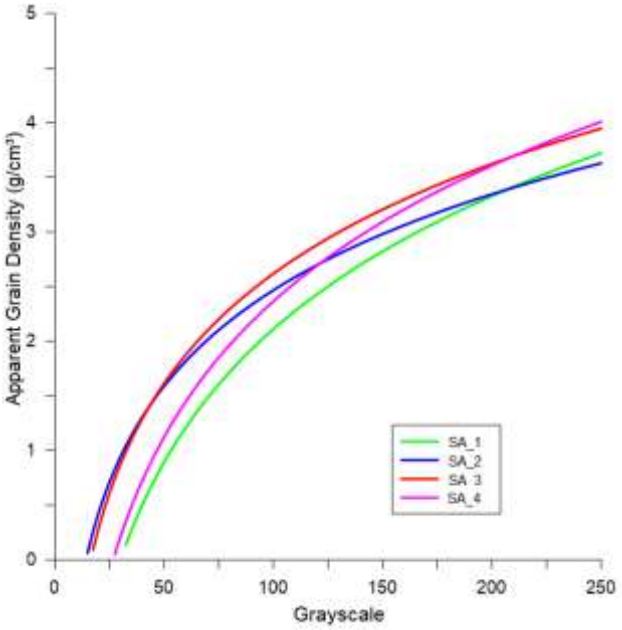

Figure 4: The four power functions generated for the four models.

Table 1: Coefficient of determination for the fit by a power function between grain density and grayscale for the four analyzed subsamples.

Subsample	R^2
SA_1	0,999
SA_2	0,996
SA_3	0,998
SA_4	0,981

The presented results show the high coefficient of determination (maximum value is 1), indicating a high degree of the function adjustment. Due to it is the same rock type, the functions of non-linear adjustment are close, but not exactly the same, because of granulometric differences between the subsamples.

The power functions found allowed the identification of the five phases present: (1) pore, (2) organic matter, (3) clay, (4) aragonite and (5) limonite. Figure 5 shows the 5 phases in a slice of the sample SA_2 (vertical), visualized with the Ortho Slice tool.

The limonite phase occurs in association with aragonite. This infers that there is a process of substitution of one by the other.

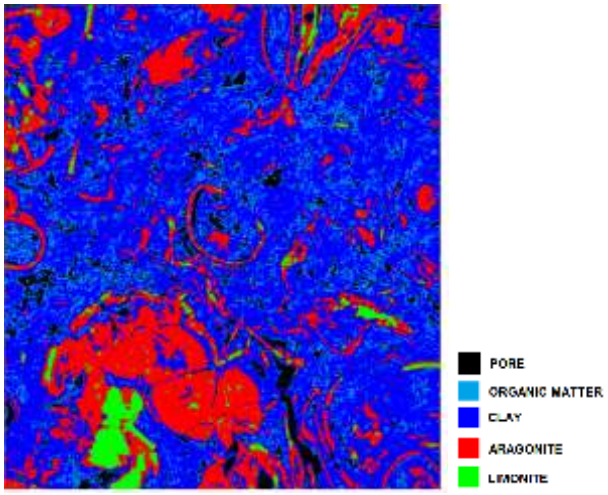

Figure 5: Phases identification for subsample SA_2.

Applying the pixel counts obtained by the Material Statistics tool, Table (2) was elaborated with the volumetric fractions of the 5 phases, for all analyzed subsamples. As would be expected for shales, clay represents the major constituent in almost all results. The only result which clay does not constituent the main part was subsample SA_3, in which the volumetric fraction of organic matter is higher than for clay.

Table 2: Results obtained for volumetric fraction of each sub-sample.

	Volumetric Fraction (%)				
	Pore	Org. Matter	Clay	Aragonite	Limonite
SA_1	9,9	27,0	51,5	11,0	0,7
SA_2	10,1	15,2	59,9	12,9	2,0
SA_3	18,3	37,3	28,5	14,7	1,2
SA_4	14,3	30,4	35,8	18,4	1,1

In addition, it is noted that the volumetric fraction values of organic matter are quite high for all rock samples. Black shales with organic contents above 20% are difficult to find (Tourtelot, 1979). For the calculation of the actual density of grains, the contribution relative to organic matter and pore was excluded, the volumetric fractions of the mineral phases were recalculated, that is, the volume considered to determine this density corresponds only to the mineral matrix.

The data generated provided the construction of Table 3 for purposes of comparison between the two grain densities for all subsamples. Due to the high content of organic matter (low density material), the sample SA_3 has the lowest apparent density value, unlike the actual density, whose horizontal samples SA_3 and SA_4 indicate the highest values. The values found for the actual grain density of the shale samples analyzed in this work are within the range of values listed in literature for the same lithology.

Table 3: Results for apparent and actual grain density for all subsamples.

	Grain Density (g/cm³)	
	Apparent	Actual
SA_1	2,004	2,305
SA_2	2,152	2,326
SA_3	1,929	2,456
SA_4	2,049	2,461

Figure (6) shows the comparison between the computational and conventional values. The values obtained by the two methods are close, indicating the reliability of the results.

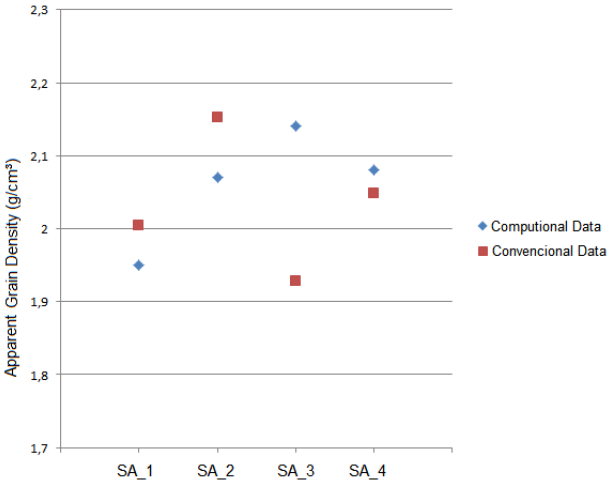

Figura 6: Comparison between computational and conventional results for grain density.

To analyze the porous phase, it was generated a surface that provided the visualization of the pores geometry, using the subsample SA_2. As would be expected to shales, it was identified planar character in the porous volumes, located between the shale layers. Futhermore, there was an evidence of moldic porosity within some aragonite shells in the microtomograpgy images. These analysis can be observed in Figure (7).

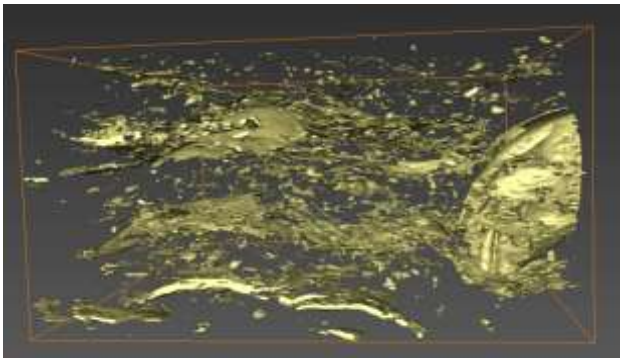

Figure 7: Porous volume of the subsample SA_2.

Conclusions

This work presents a new method for the evaluation of the mineral composition and the actual grain density of rocks samples from the analysis of the images obtained in x-ray microtomography tests. In this case, the proposed methodology was applied to four samples of black shale extracted from the Araripe Basin.

The mineral composition analysis indicated the occurrence of high organic matter and clay minerals, as well as a considerable volumetric fraction composed of carbonate shells formed by the aragonite mineral, with possible partial replacement by the limonite mineral (trace). The high levels of organic matter present in black shales of the Araripe Basin led to the conclusion that they have potential for the generation and accumulation of hydrocarbons, constituting in conventional non-conventional reservoirs.

The apparent grain densities identified in three of the four analyzed samples were close to those measured in the laboratory and the actual grain densities are compatible with values listed in the literature for shales.

The microtomographic images show the planar character of the phases that compose the shale samples, including most of their porous spaces.

References

BATISTA, J. T.; SOARES, J. A. (2016). **Petrofísica de folhelhos negros da Bacia Do Araripe.** Centro de Ciências e Tecnologia. Universidade Federal de Campina Grande, Campina Grande.

CHAGAS, D. B. (2006). **Litoestratigrafia da Bacia do Araripe: reavaliação e propostas para revisão.** 112 f. Dissertação (Mestrado em Geociências). Instituto de Geociências e Ciências Exatas. Universidade Estadual Paulista, Rio Claro.

PORTO, A. L. (2015). **Estimação de propriedades petrofísicas de rochas sedimentares a partir de imagens microtomográficas de raios-X.** 122 f. Tese (Doutorado em Engenharia de Processos). Centro de Ciências e Tecnologia. Universidade Federal de Campina Grande, Campina Grande.

RIBEIRO, T. J. S. (2015). **Estudo de reservatórios não convencionais de *shale gas* no Brasil.** 84 f. Centro de Tecnologia. Universidade Federal do Rio Grande do Norte, Natal.

TOURTELOT, H. A. (1979). **Black shale - Its deposition and diagenesis.** U. S. Geological Survey. Clays and Clay Minerals, vol 27. Denver, Colorado.